AMERICAN SOCIETY FOR MICROBIOLOGY | Molecular and Cellular Biology®

RESEARCH ARTICLE

Inhibition of SGLT1 Alleviates the Glycemic Variability-Induced Cardiac Fibrosis via Inhibition of Activation of Macrophage and Cardiac Fibroblasts

Weihua Wu,[a] Qian Chai,[b] Ziying Zhang[b]

[a]Department of Endocrinology, Third Affiliated Hospital of Shenzhen University, Shenzhen, People's Republic of China
[b]Department of General Medicine, First Affiliated Hospital of Harbin Medical University, Harbin, People's Republic of China

ABSTRACT Glycemic variability has been considered one of the predictors of diabetes complications in patients with diabetes mellitus (DM). In this work, we evaluated whether glycemic variability induces cardiac fibrosis through regulating cardiac fibroblast activation and macrophage polarization. Moreover, we determined whether glucose transporter sodium-glucose cotransporter 1 (SGLT1) plays an important role in this process. Glycemic variability-induced mice were established using DM mice (GVDM mice), and intermittent high-glucose (IHG) treatment was used to simulate glycemic variability in RAW264.7 macrophages and cardiac fibroblasts. The short hairpin RNA for SGLT1 was used to knock down SGLT1. The results showed that glycemic variability aggravated the cardiac fibrosis in GVDM mice. Additionally, glycemic variability promoted the expression of fibrogenic cytokine and the extracellular matrix proteins in left ventricular tissues and cardiac fibroblasts. GVDM mice showed a higher incidence of macrophage infiltration and M1 polarization in left ventricular tissues. Moreover, IHG-promoted RAW264.7 macrophages tended to differentiate to M1 phenotype. SGLT1 knockdown alleviated cardiac fibrosis in GVDM mice and inhibited activations of cardiac fibroblast and macrophage M1 polarization. Our results indicated that glycemic variability aggravates cardiac fibrosis through activating cardiac fibroblast and macrophage M1 polarization, which could be partially inhibited by SGLT1 knockdown.

KEYWORDS diabetes mellitus, glycemic variability, cardiac fibrosis, SGLT1, macrophage polarization, cardiac fibroblast

Glycemic variability (GV), which refers to blood glucose fluctuations over time, has been considered a predictor of diabetes complications in patients with type 2 diabetes mellitus (T2DM) (1–4). Glycemic variability is a normal physiological process after fasting and feeding in healthy people. However, the amplitude and frequency of glycemic variability are different between people with and without diabetes (5, 6). The pathological glycemic variability in diabetic patients will lead to hyperglycemia and hypoglycemia. Therefore, glycemic variability will cause serious damage to diabetic patients compared to sustained hyperglycemia (7–10). Compared to sustained hyperglycemia, glycemic variability could aggravate oxidative stress activation and inflammation to induce tissue or cell pathology (11, 12). Glycemic variability contributes to many diabetes complications such as renal injury in diabetic rats and diabetic retinopathy in patients with T2DM (13, 14). However, the investigations of glycemic variability on diabetic cardiopathy are limited. A study found that high glycemic variability aggravates left ventricular diastolic function of T2DM patients, and the authors pointed that reduction of glycemic variability might improve heart failure with preserved ejection fraction (HFpEF) (15). Additionally, it has been reported that glycemic variability promotes

Address correspondence to Weihua Wu, wwh_2678@163.com.

The authors declare no conflict of interest.

Received 16 June 2021
Returned for modification 30 June 2021
Accepted 19 November 2021

Accepted manuscript posted online 29 November 2021
Published 17 February 2022

cardiac fibrosis in diabetic rats (16). However, the effects of glycemic variability on diabetic cardiopathy in murine model and the underlying regulatory mechanisms are still unclear. In this study, we assessed the effects of glycemic variability on cardiac fibrosis in diabetic mice and tried to reveal the potential regulatory mechanism.

Cardiac fibrosis is a pathological process to form and deposit fibrotic extracellular matrix (ECM) and can lead to adverse cardiac remodeling. Cardiac fibrosis also is an important pathological feature in many cardiovascular diseases, including heart failure, myocardial infarction, and hypertensive heart diseases (17–19). Additionally, studies found that cardiac fibrosis is related to the development of diabetic cardiomyopathy and cardiac hypertrophy (20, 21). In diabetes, hyperglycemia increases the expression of fibrogenic cytokine transforming growth factor β (TGF-β) in cardiac fibroblasts, which leads to cardiac fibrosis (20). Moreover, high glucose (HG) could promote cell proliferation of cardiac fibroblasts and upregulate the protein expression of fibrillar collagens *in vitro* (22, 23). Macrophage, a type of immune cell, could regulate inflammation in cardiovascular and hypertension diseases (24, 25). Macrophage recruitment and polarization are the important processes for cardiac fibrosis (26). Under certain pathophysiologic conditions, macrophages undergo phenotypic polarization. Two major types of macrophages are classically activated macrophages (M1) and alternatively activated macrophages (M2) (27). M1 macrophages are proinflammatory macrophages, producing proinflammatory factors, which then leads to induction of inflammation and cardiac fibrosis (26). M2 macrophages are considered anti-inflammatory macrophages, and replacing M1 macrophages with M2 macrophages could inhibit cardiac fibrosis (28). In this study, we evaluated whether glycemic variability could promote cardiac fibrosis by regulating activation of cardiac fibroblasts and macrophages.

Sodium-glucose cotransporters SGLT1 (encoded by solute carrier family 5 member 1 *SLC5A1*) and SGLT2 (encoded by *SLC5A2*) are key glucose transport mediators crossing to the cell membrane. SGLT2 is specifically expressed in human and mouse kidney. SGLT1, on the other hand, is expressed in various organs such as heart, kidney, liver, and small intestine both in humans and in mice (29–31). Importantly, it has been reported that SGLT1 is highly expressed in human and murine hearts (31, 32). Knockout of SGLT1 in mice could abolish chronic pressure overload-caused cardiac hypertrophy and fibrosis (33). Moreover, SGLT1, not SGLT2, has been proved to be involved in HG-induced matrix metalloproteinase2 (MMP-2) expression, a profibrotic factor, in human cardiac fibroblasts (34). The mRNA expression of SGLT1 in heart is significantly increased both in patients with T2DM and coronary artery disease and in animal models (35). In addition, SGLT1 is upregulated in human myocardial tissue under ischemia and hypertrophy conditions (36). Furthermore, a selective SGLT1 inhibitor KGA-2727 inhibits the myocardial infarction-induced left ventricular hypertrophy and fibrosis in mice (37). Therefore, in this study, we induced glycemic variability and inhibited SGLT1 expression by knocking down SGLT1 to investigate whether SGLT1 plays an important role in glycemic variability-induced mice. It might be very helpful to better understand the underlying mechanism of cardiac fibrosis.

RESULTS

Glycemic variability-induced cardiac dysfunction is abrogated by SGLT1 inhibition. The blood glucose levels 30 min after insulin and glucose injection were measured in week 13. The glucose level and glucose fluctuation in week 13 showed that the glycemic variability was induced by alternate insulin and glucose injections, and knockdown of SGLT1 reduced the glycemic variability in week 13 (Fig. 1A and B). Next, the cardiac dysfunction was monitored, and the results showed that glycemic variability aggravated cardiac dysfunction by suppressing the ejection fraction (EF) and fractional shortening (FS) and enhanced the left ventricular end-diastolic dimension (LVEDd) and left ventricular end-systolic dimension (LVESd) (Fig. 1C to F). Additionally, the cardiac dysfunction in GVDM mice seemed more serious than in diabetes mellitus (DM) mice. However, the results showed that SGLT1 inhibition in GVDM mice ameliorated the cardiac dysfunction judging by reversing the changes of these parameters.

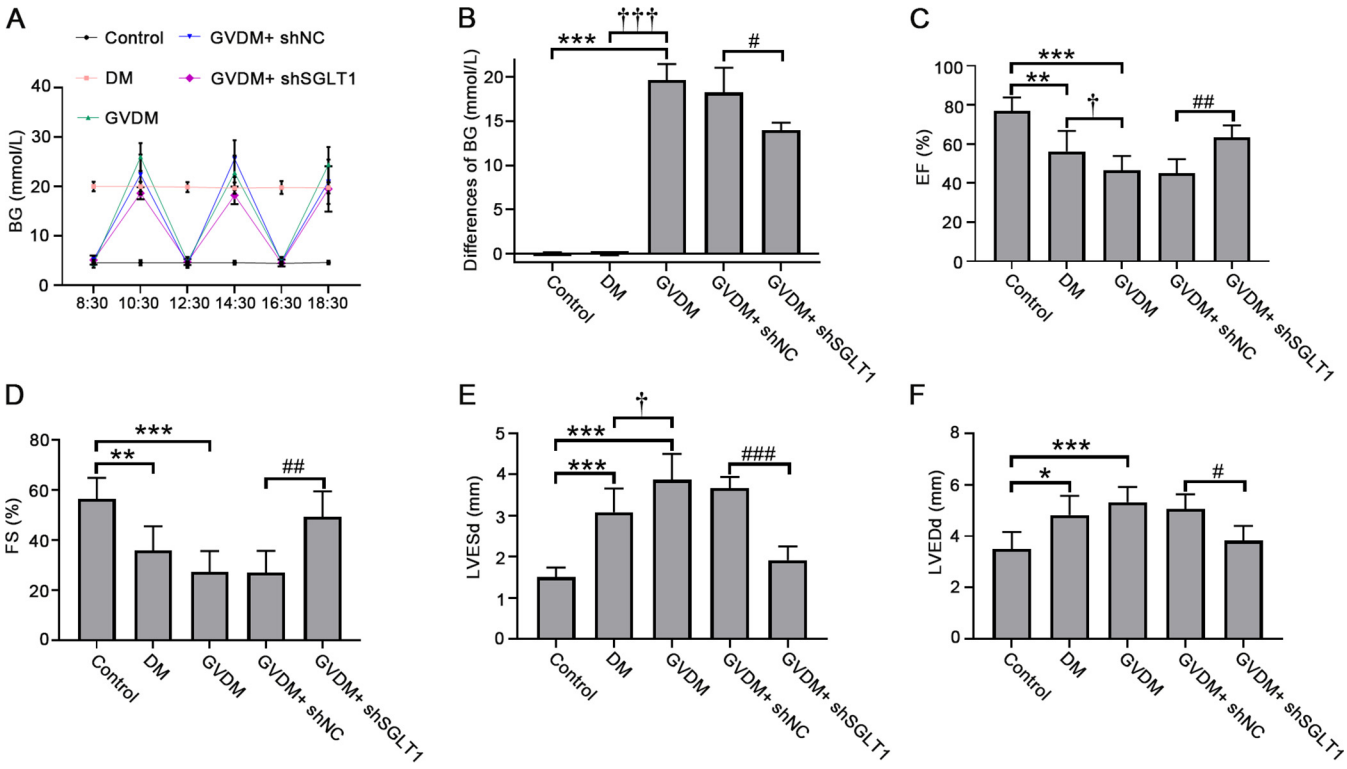

FIG 1 Glycemic variability-induced cardiac dysfunction is abrogated by SGLT1 inhibition. (A) The blood glucose (BG) levels of mice 30 min after insulin or glucose injection at each time point in week 13. (B) The average differences of glucose levels 30 min after insulin and glucose treatment in week 13. (C to F) The cardiac parameters left ventricular ejection fraction (EF), fractional shortening (FS), left ventricular end-systolic dimension (LVESd), and left ventricular end-diastolic dimension (LVEDd) were measured by echocardiography. The data are expressed as means ± standard deviation (SD) (n = 6/group). ***, $P < 0.001$; **, $P < 0.01$; *, $P < 0.05$ versus control mice. †††, $P < 0.001$; †, $P < 0.05$ versus DM mice. ###, $P < 0.001$; ##, $P < 0.01$; #, $P < 0.05$ versus GVDM + shNC mice. DM, diabetes mellitus; GV, glycemic variability; SGLT1, sodium-glucose cotransporter 1; shSGLT1, SGLT1 short hairpin RNA; shNC, negative-control short hairpin RNA.

Glycemic variability-aggravated cardiac fibrosis is alleviated by SGLT1 inhibition. The mRNA and protein levels of SGLT1 in left ventricular tissues of mice were detected to confirm that SGLT1 was silenced by short hairpin RNA (shRNA) against SGLT1. Our results showed that knockdown of SGLT1 clearly reduced the increased expression of SGLT1 by glycemic variability (Fig. 2A to C). Next, the effects of glycemic variability on cardiac fibrosis were determined. In the results of Masson's trichrome staining, the fibrotic area of left ventricular tissues in GVDM mice was increased dramatically compared with that in the control and DM group mice. The degree of fibrosis was reduced in SGLT1 shRNA-treated mice (Fig. 2D and E). Moreover, we found that the fibrogenic cytokine TGF-β1 and the ECM proteins such as fibronectin, α-smooth muscle actin (α-SMA), collagen I, and collagen III were significantly upregulated in DM mice and had higher levels than in GVDM mice, and inhibition of SGLT1 clearly downregulated expression of these factors in GVDM mice (Fig. 3A to G). Additionally, the expression of collagen III was also confirmed by immunohistochemical staining. The staining results of collagen III were consistent with its protein expression analysis (Fig. 3H and I). Our results indicated that glycemic variability aggravates cardiac fibrosis and that SGLT1 inhibition could alleviate glycemic variability-caused cardiac fibrosis.

Glycemic variability drives M1 macrophage polarization and inhibition of SGLT1 promotes macrophages toward a M2 phenotype in GVDM mice. In order to verify whether glycemic variability drives M1 macrophage polarization, M1 and M2 macrophage polarization were analyzed by gene marker expression using quantitative reverse transcription (qRT)-PCR and immunofluorescence assay. The mRNA levels of M1 markers monocyte chemotactic protein-1 (MCP-1) and CD86 and M2 marker CD206 in left ventricular tissues were measured. The results showed that expression of MCP-1 and CD86 was increased in the DM and GVDM groups, and the expression levels were much

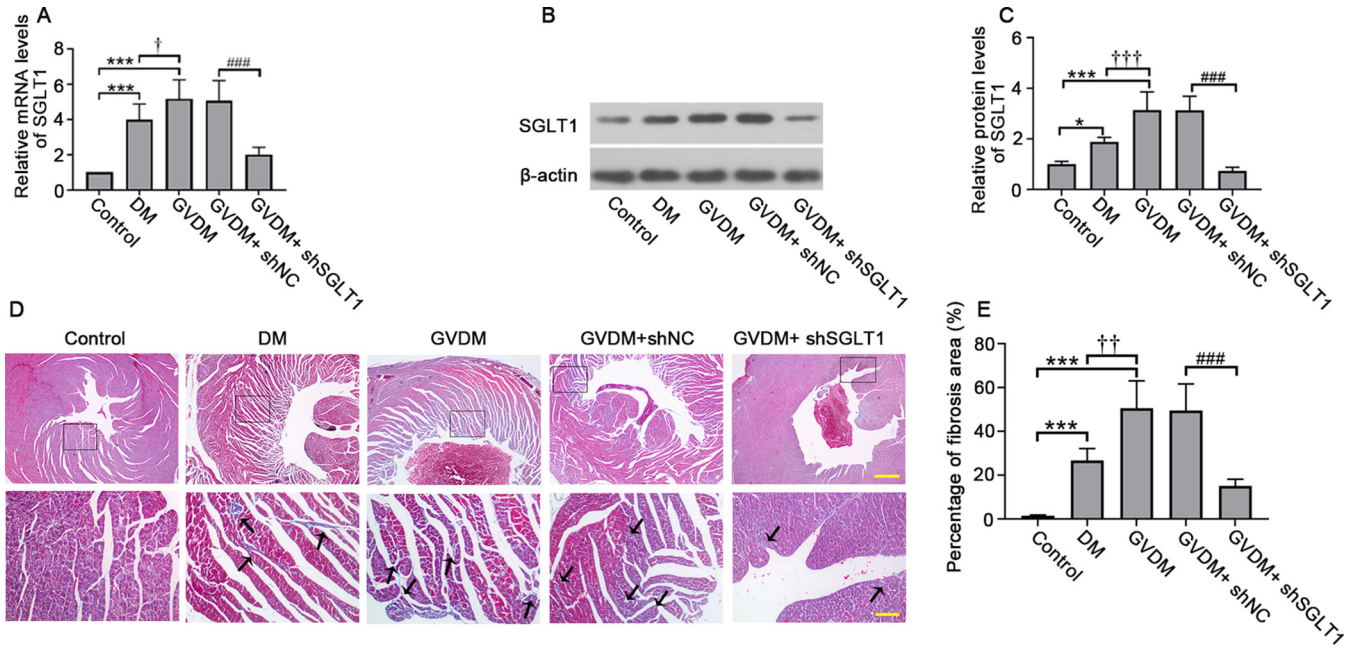

FIG 2 Glycemic variability-aggravated cardiac fibrosis is alleviated by SGLT1 inhibition. (A) The relative mRNA expression of SGLT1 in left ventricular tissues were detected by qRT-PCR. (B) The protein levels of SGLT1 in left ventricular tissues were detected by Western blot. (C) Quantitative analysis of the protein levels of SGLT1. (D) The cardiac fibrosis was determined by Masson's trichrome staining. Scale bars, 500 (upper panel) and 100 (lower panel) μm. The arrows point to Aniline Blue. (E) The percentage of fibrosis area in total staining area (six mice/group, three sections/mouse). The data are expressed as means ± SD (n = 6/group). ***, $P < 0.001$ versus control mice. †††, $P < 0.001$; ††, $P < 0.01$; †, $P < 0.05$ versus DM mice. ###, $P < 0.001$ versus GVDM + shNC mice.

higher in the GVDM group (Fig. 4A and B). Knockdown of SGLT1 remarkably reduced the expression of MCP-1 and CD86 compared to shNC-treated mice. Additionally, CD206 was decreased in the GVDM group, and SGLT1 inhibition dramatically enhanced CD206 expression in left ventricular tissues (Fig. 4C). Moreover, the percentages of M1 (Green-CD68$^+$, Red-iNOS$^+$) and M2 (Green-CD68$^+$, Red-Arg-1$^+$) macrophages were examined by double-immunofluorescence staining (Fig. 4D to G). The results showed that there were more CD68-positive cells aggregated in left ventricular tissues of GVDM mice than that in control and DM mice. The iNOS$^+$/CD68$^+$ M1 macrophages were increased in GVDM groups compared to control and DM mice, but they were significantly reduced by SGLT1 silence. Conversely, the percentages of Arg-1$^+$/CD68$^+$ M2 macrophages were prominently increased in SGLT1-inhibited mice. The results indicated that glycemic variability aggravates macrophage infiltration and drives more macrophages into M1 phenotype compared to control and DM mice. Inhibition of SGLT1 partially reverses the M1 macrophage polarization and significantly promotes macrophages toward a M2 phenotype in left ventricular tissues of GVDM mice.

SGLT1 is downregulated in cardiac macrophages and fibroblasts of GVDM mice that received shSGLT1. In this study, we confirmed that SGLT1 is expressed in various organs such as the heart, liver, kidney, and small intestine of mice (Fig. 5A and B). Then we detected the expression of SGLT2 in kidney and the expression of SGLT1 in the heart, liver, kidney, and small intestine of mice that received shSGLT1 or shNC. The results showed that shSGLT1 did not affect SGLT2 expression in kidney and shSGLT1 silenced SGLT1 expression in the kidney, heart, intestine, and liver, and the gene silencing efficiency of shSGLT1 was higher in the heart (Fig. 5C to H). Next, double immunofluorescence was performed to verify whether SGLT1 expresses in macrophages and fibroblasts and whether shSGLT1 could silence SGLT1 expression in macrophages and fibroblasts under GVDM condition. We found that in control mice, SGLT1 is expressed in macrophages and fibroblasts. More double-staining cells were shown in GVDM + shNC mice. More importantly, shSGLT1 injection decreased the SGLT1 expression in macrophages and fibroblasts (Fig. 5I and J). Our results indicated that SGLT1 may affect glycemic variability-induced cardiac fibrosis, at least partly, via directly regulating the activation of macrophages and fibroblasts in heart.

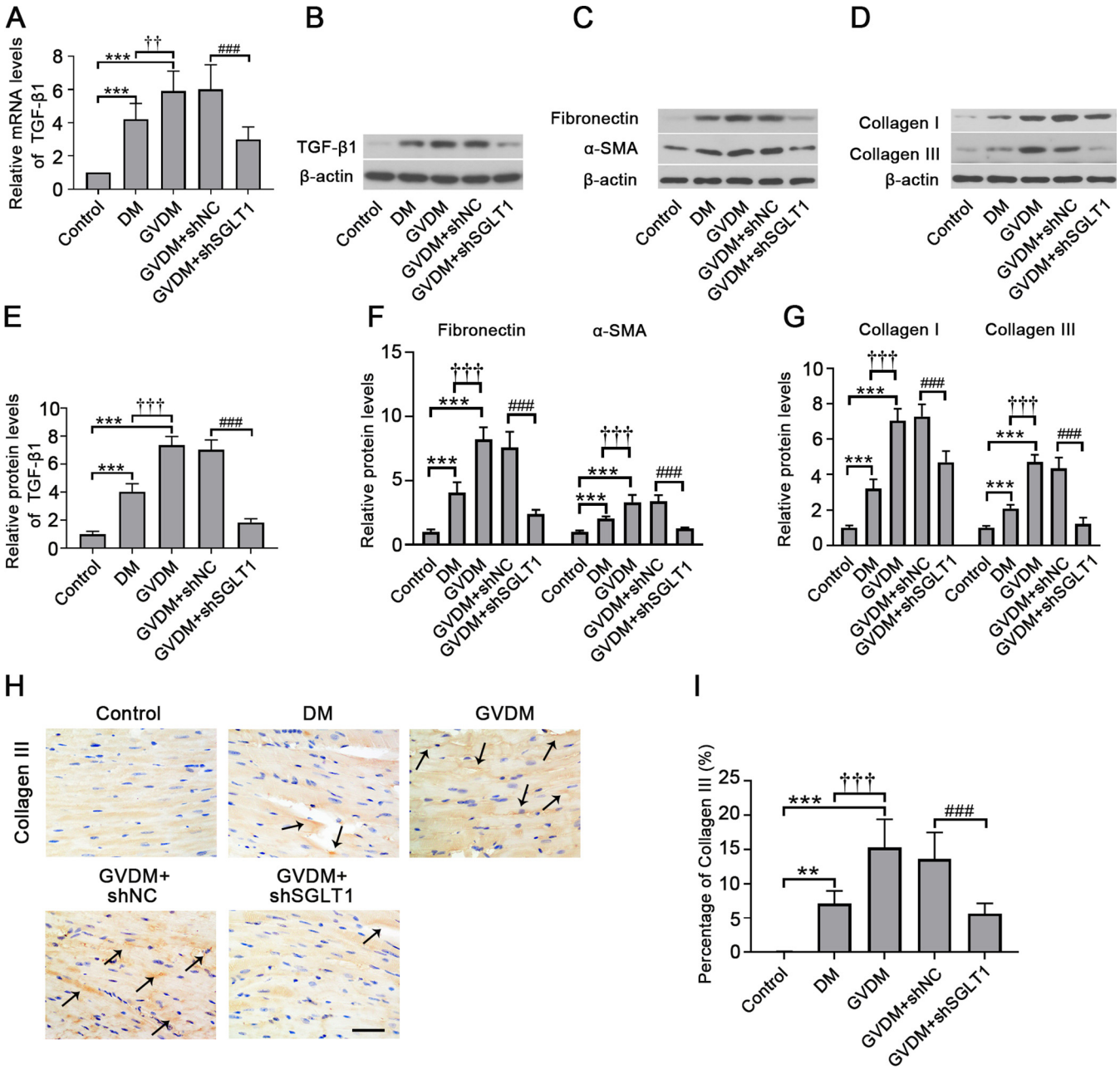

FIG 3 Glycemic variability-upregulated expression of fibrogenic cytokine TGF-β1 and extracellular matrix proteins are alleviated by SGLT1 inhibition. (A) The relative mRNA expression of TGF-β1 in left ventricular tissues were detected by quantitative reverse transcription (qRT)-PCR. (B) The protein levels of TGF-β1 in left ventricular tissues were detected by Western blot. (C to D) The protein levels of fibronectin and α-SMA, collagen I, and collagen III in left ventricular tissues were detected by Western blot. (E to G) Quantitative analysis of the protein levels of TGF-β1, fibronectin, α-SMA, collagen I, and collagen III. (H) The expression of collagen III was detected by immunohistochemical analysis. Scale bar, 50 μm. Arrows point to collagen III. (I) The percentage of collagen III staining area in total staining area (%) (six mice/group, three sections/mouse). The data are expressed as means $\pm$ SD (n = 6/group). ***, $P < 0.001$; **, $P < 0.01$ versus control mice. †††, $P < 0.001$; ††, $P < 0.01$ versus DM mice. ###, $P < 0.001$ versus GVDM + shNC mice. TGF-β1, transforming growth factor β1; α-SMA, α-smooth muscle actin.

Inhibition of SGLT1 inhibits cardiac fibroblast proliferation and activation in IHG-treated cardiac fibroblasts. The cardiac fibroblasts were isolated from mice, and cell identification was performed by staining vimentin (38). The results showed that most of the cells on the third passage expressed vimentin, and high purity of cardiac fibroblast was obtained (Fig. 6A). Subsequently, the IHG model was induced by alternately normal glucose (NG) and high-glucose (HG) treatment, and lentiviral vector containing shSGLT1 was used to silence SGLT1 protein. The results showed that both the mRNA and protein levels of SGLT1 were decreased in shSGLT1-received cells (Fig. 6B to D). Then cell

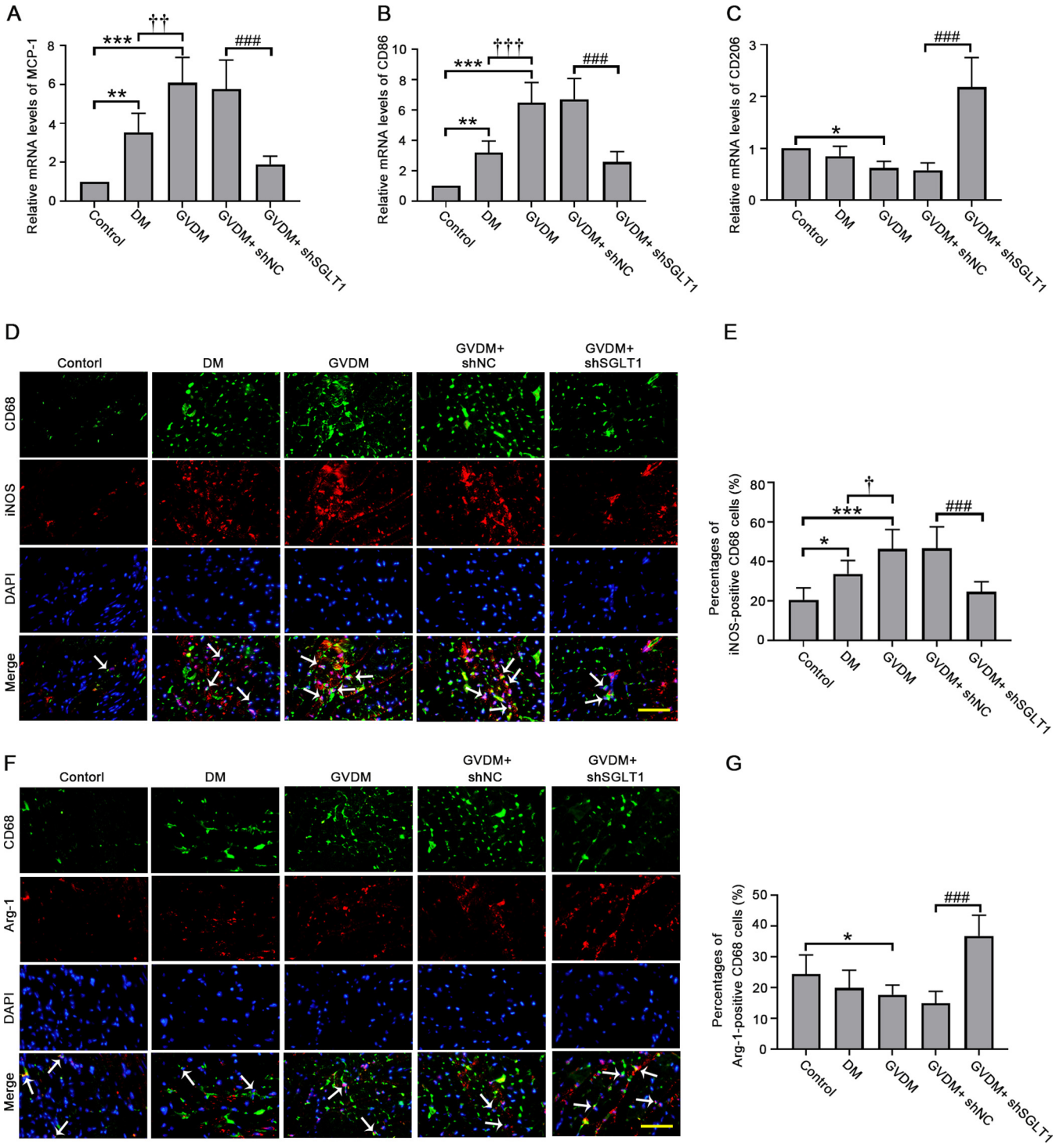

FIG 4 Glycemic variability drives macrophage infiltration and M1 polarization, and inhibition of SGLT1 promotes macrophages toward a M2 phenotype in GVDM mice. (A to C) The relative mRNA expression of MCP-1, CD86, and CD206 in left ventricular tissues was detected by qRT-PCR. (D and F) The contents of M1 ($CD68^+$, $iNOS^+$) and M2 ($CD68^+$, $Arg\text{-}1^+$) macrophages were examined by double-immunofluorescence staining. Scale bars, 50 μm. Arrows point to double-immunofluorescence staining cells. (E and G) The percentage of iNOS-positive CD68 macrophages and the percentage of Arg-1-positive CD68 macrophages (six mice/group, three sections/mouse). The data are expressed as means ± SD ($n = 6$/group). ***, $P < 0.001$; **, $P < 0.01$; *, $P < 0.05$ versus control mice. †††, $P < 0.001$; ††, $P < 0.01$; †, $P < 0.05$ versus DM mice. ###, $P < 0.001$ versus GVDM + shNC mice. Arg-1, arginase 1; DAPI, 4',6-diamidino-2-phenylindole; iNOS, inducible nitric-oxide synthase.

proliferation of cardiac fibroblasts was measured, and the results displayed that HG and IHG treatment could promote cell proliferation of cardiac fibroblasts and showed a higher proliferative ability in IHG group. We also found that knockdown of SGLT1 suppressed cell proliferation in IHG-treated cells (Fig. 6E). In addition, we found that IHG promoted

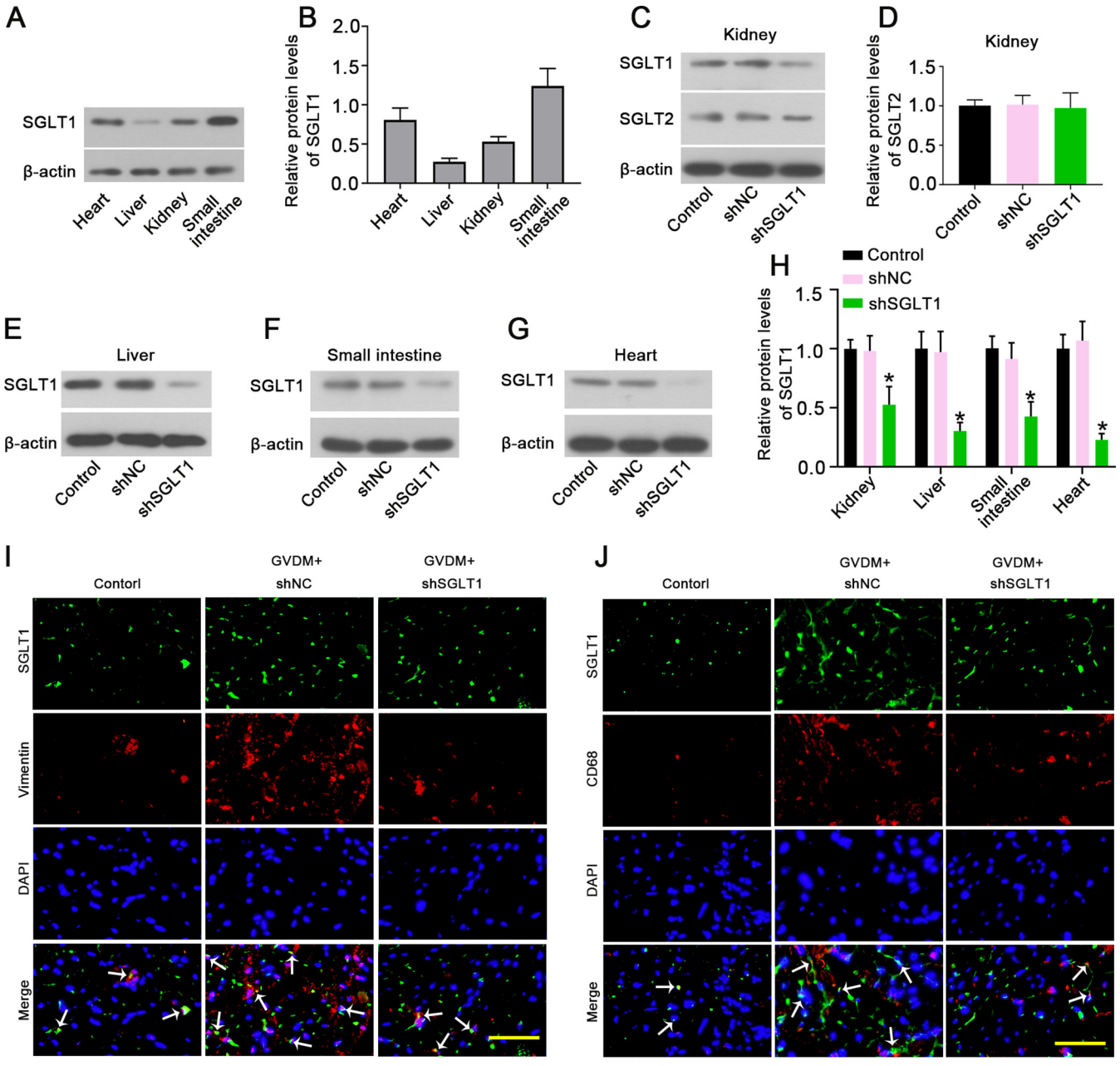

FIG 5 SGLT1 is downregulated in cardiac macrophages, and fibroblasts of GVDM mice received shSGLT1. (A) The protein levels of SGLT1 in heart, liver, kidney, and small intestine were detected by Western blot. (B) Quantitative analysis of the protein levels of SGLT1. (C) C57BL/6 mice received with AAV9-mediated shSGLT1 or shNC for 4 weeks. The protein levels of SGLT1 and SGLT2 in kidney were detected by Western blot. (D) Quantitative analysis of the protein levels of SGLT2 in kidney. (E to G) The protein levels of SGLT1 in liver, small intestine, and heart were detected by Western blot. (H) Quantitative analysis of the protein levels of SGLT1 in heart, liver, kidney, and small intestine. The data are expressed as means ± SD (n = 6/group). *, $P < 0.05$ versus shNC mice. (I and J) The expression of SGLT1 and vimentin, SGLT1, and CD68 in left ventricular tissues were examined by double-immunofluorescence staining. Scale bars, 50 μm (n = 6/group). Arrows point to double-immunofluorescence staining cells.

the expression of TGF-β1, collagen I, and collagen III (Fig. 6F to I). However, inhibition of SGLT1 observably suppressed the enhanced TGF-β1, collagen I, and collagen III that induced by IHG.

IHG stimulates macrophage polarization, and inhibition of SGLT1 promotes M2 macrophage polarization. The effects of IHG on macrophage polarization were assessed in RAW264.7 cells *in vitro*. First, the expression of SGLT1 was detected in IHG-induced and SGLT1-inhibited RAW264.7 cells. The results showed that IHG significantly upregulated SGLT1 mRNA and protein expression compared to NG- and HG-treated

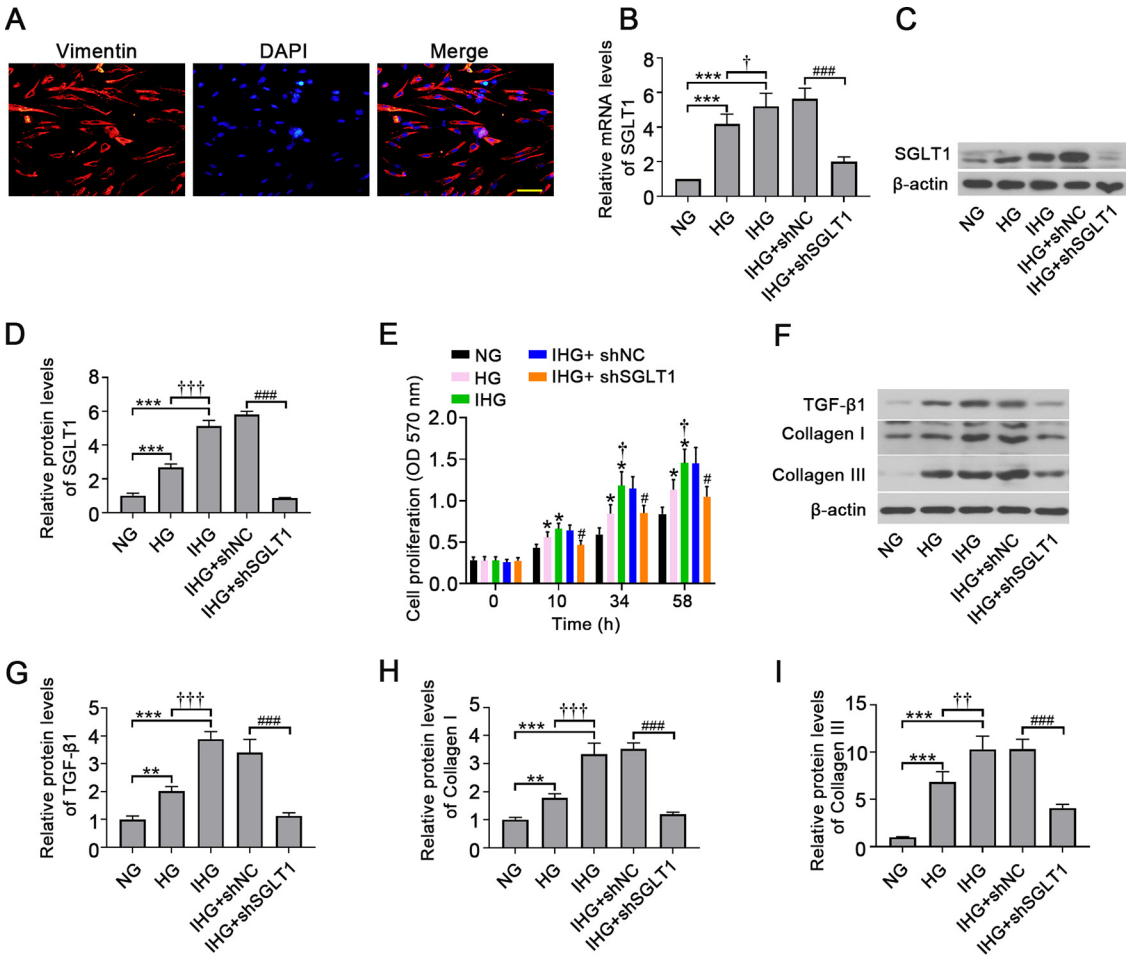

FIG 6 Inhibition of SGLT1 inhibits cardiac fibroblast proliferation and activation in IHG-treated cardiac fibroblasts. (A) Cell identification of cardiac fibroblasts was determined by vimentin expression. Scale bar, 50 μm. (B) The relative mRNA expression of SGLT1 in cardiac fibroblasts were detected by qRT-PCR. (C) The protein levels of SGLT1 in cardiac fibroblasts were detected by Western blot. (D) Quantitative analysis of the protein levels of SGLT1. (E) The cell proliferation of cardiac fibroblasts was detected by 3-(4,5-dimethylthiazol-2-yl)-2,5-diphenyltetrazolium bromide (MTT). (F) The protein levels of TGF-β1, collagen I, and collagen III in cardiac fibroblasts were detected by Western blot. (G to I) Quantitative analysis of the protein levels of TGF-β1, collagen I, and collagen III. The data are expressed as means ± SD (n = 3/group). ***, $P < 0.001$; **, $P < 0.01$; *, $P < 0.05$ versus NG. †††, $P < 0.001$; ††, $P < 0.01$; †, $P < 0.05$ versus HG. ###, $P < 0.001$; #, $P < 0.05$ versus IHG + shNC. NG, normal glucose; HG, high glucose; IHG, intermittent high glucose.

cells, and knockdown of SGLT1 partially inhibited IHG-increased SGLT1 expression (Fig. 7A to C). The macrophage M1 markers MCP-1, CD86, and nitric-oxide synthase (iNOS) were increased in HG- and IHG-treated cells, and they had higher levels in IHG-treated cells. Inhibition of SGLT1 partially downregulated IHG increased the expression of macrophage M1 markers (Fig. 7D to F). However, IHG decreased macrophage M2 markers CD206 and Arg-1, and knockdown of SGLT1 dramatically enhanced M2 macrophage percentages determined by the enhanced expression of CD206 and Arg-1 (Fig. 7G and H). The results indicated that IHG stimulates M1 macrophage polarization and could be suppressed by inhibition of SGLT1. Moreover, inhibition of SGLT1 benefits macrophage toward M2 phenotype in IHG-treated cells.

DISCUSSION

Cardiac dysfunction is an important feature in many heart-related diseases such as heart failure, myocardial infarction, and diabetic cardiomyopathy (39–41). Our results show that, compared to sustained hyperglycemia, glycemic variability aggravated the cardiac dysfunction of GVDM mice characterized by decreases of LVEF and increases of

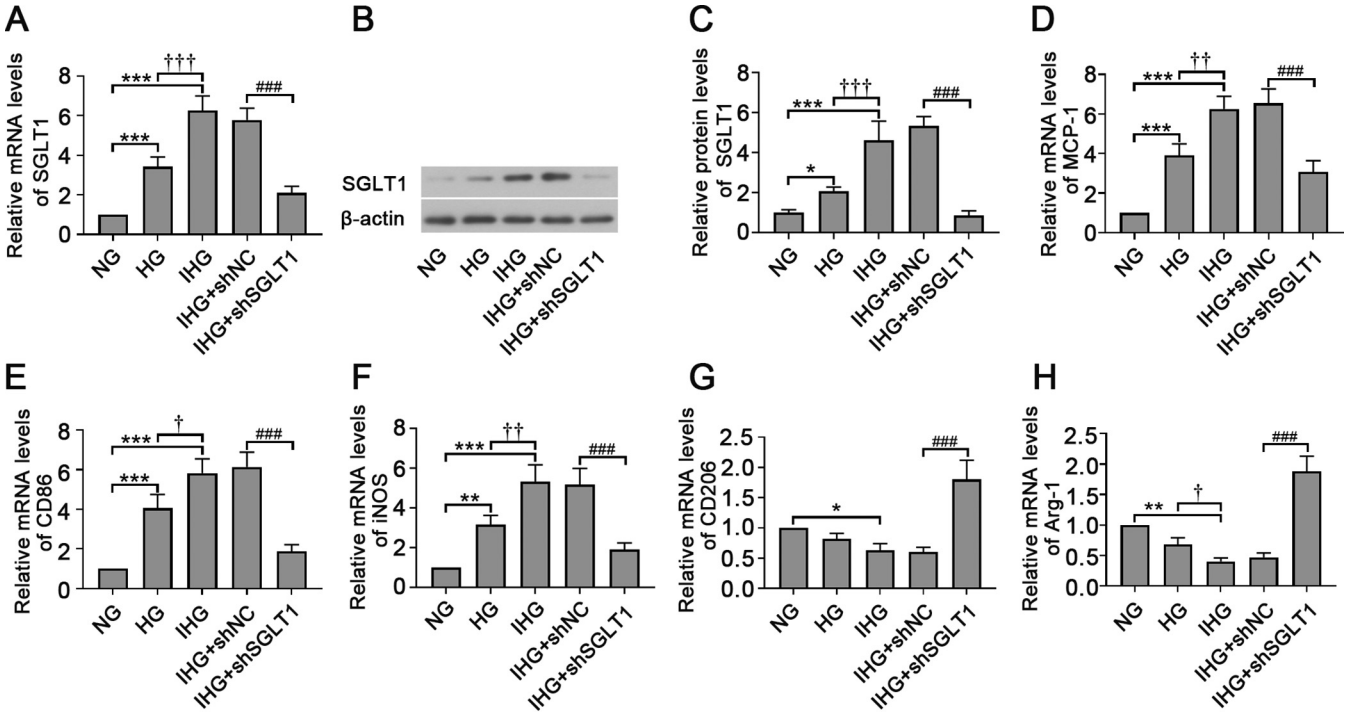

FIG 7 IHG stimulates macrophage M1 polarization and inhibition of SGLT1 promotes M2 macrophage polarization. (A) The relative mRNA expression of SGLT1 in RAW264.7 cells was detected by qRT-PCR. (B) The protein levels of SGLT1 in RAW264.7 cells were detected by Western blot. (C) Quantitative analysis of the protein levels of SGLT1. (D to H) The relative mRNA expression of MCP-1, CD86, iNOS, CD206, and Arg-1 in RAW264.7 cells was detected by qRT-PCR. The data are expressed as means ± SD (n = 3/group). ***, $P < 0.001$; **, $P < 0.01$; *, $P < 0.05$ versus NG. †††, $P < 0.001$; ††, $P < 0.01$; †, $P < 0.05$ versus HG. ###, $P < 0.001$ versus IHG + shNC.

LVESd. Our results were consistent with the previous reports by others that glycemic variability could aggravate cardiac dysfunction (15, 42). Moreover, in our study, we found that the effects of glycemic variability on cardiac dysfunction were alleviated in SGLT1-inhibited mice.

Under cardiac pathophysiologic conditions, cardiac fibrosis commonly occurs by expressing and accumulating ECM proteins in cardiac interstitium, which leads to destroying the normal cardiac structure and impairing cardiac function (43, 44). Therefore, cardiac fibrosis is an important process for contributing to heart injury. Our results showed that glycemic variability increased the fibrosis areas and promoted the expression of TGF-β1, fibronectin, α-SMA, collagen I, and collagen III in the left ventricle tissues compared to DM mice. We also found that IHG promoted the cell proliferation and the expression of TGF-β1, collagen I and collagen III compared to HG-treated cardiac fibroblasts *in vitro*. In heart, cardiac fibroblasts play the important roles in dedicating to myocardial structure and cell signaling in heart (38). However, it is well known that activation of cardiac fibroblasts contributes to the process of cardiac fibrosis. Cardiac fibroblasts have high proliferative ability and are able to regulate the synthesis of ECM proteins, such as fibronectin, collagen I, and collagen III (23, 38, 45). Moreover, cardiac fibroblasts could be stimulated by profibrosis gene TGF-β1 to undergo conversion to myofibroblasts, and myofibroblast is the main effector cell for cardiac fibrosis (20, 38). Studies found that TGF-β1/Smad2/3 pathway in cardiac fibroblasts is involved in promoting cardiac fibrosis (46, 47). Moreover, TGF-β1 upregulates the expression of collagen I and collagen III in cardiac fibroblasts (48, 49). In HG-treated cardiac fibroblasts, the expression of TGF-β1, collagen I, and collagen III is increased in cardiac fibroblasts, and HG favors proliferation of cardiac fibroblasts (50, 51). Therefore, our results indicated that glycemic variability might promote cardiac fibrosis by activation of cardiac fibroblasts. Our results showed that SGLT1 was expressed in fibroblast in left ventricular tissue, and knockdown of SGLT1 decreased the SGLT1 expression in

fibroblasts in GVDM + shSGLT1 mice. Moreover, our results show that inhibition of SGLT1 could reduce the increased expression of TGF-β1, collagen I, and collagen III in left ventricular tissues and fibroblasts and inhibit the IHG-induced the increases of proliferation of cardiac fibroblasts. Thus, our results indicated that the effects of glycemic variability on cardiac fibroblasts might be partially regulated by SGLT1 in cardiac fibroblasts.

Next, we detected the macrophage infiltration and polarization in the left ventricular tissues. The results showed that compared with DM mice, glycemic variability increased the content of CD68-positive macrophages, indicating that glycemic variability promoted the macrophage infiltration in the left ventricular tissues. We also found that glycemic variability promoted the expression of MCP-1 in left ventricular tissues. MCP-1 is an important proinflammatory and profibrotic factor that is released by parenchymal cells and macrophages. MCP-1 is a chemokine attracting macrophages to the injured tissue, and it is able to directly promote the activation of fibroblasts (43, 52–54). Additionally, MCP-1 could be secreted by proinflammatory macrophages such as M1 macrophages to maintain the inflammatory state in injured tissues (55). Our results showed that glycemic variability increased the expression of M1 markers CD86 and iNOS in left ventricular tissues. Moreover, IHG significantly increased MCP-1, CD86, and iNOS expression in RAW264.7 cells compared to HG-treated cells *in vitro*. This indicated that glycemic variability promotes macrophages to differentiate into proinflammatory M1 macrophages. We also found that knockdown of SGLT1 inhibited CD86 expression and reduced the iNOS-positive macrophages in left ventricular tissues. Inhibition of SGLT1 dramatically enhanced anti-inflammatory macrophage M2 marker CD206 expression and the percentage of Arg-1-positive macrophages in GVDM-shSGLT1 mice. Moreover, we found that SGLT1 was expressed in macrophages in left ventricular tissues, and knockdown of SGLT1 decreased the SGLT1 expression in macrophages in GVDM + shSGLT1 mice. *In vitro*, RAW264.7 macrophages tended to differentiate to the M1 phenotype in IHG-treated cells, and inhibition of SGLT1 promoted macrophages to switch from the M1 to M2 phenotype. Our results indicated that inhibition of SGLT1 suppresses glycemic variability-induced macrophage M1 polarization, which might inhibit the inflammatory response in heart and then improve cardiac fibrosis.

It has been reported that compared with sustained hyperglycemia, glycemic variability exacerbates inflammation in patients with T2DM (11, 56). SGLT1 is a glucose transport mediator, and it can regulate cell glucose absorption. It has been reported that SGLT1 is expressed in the human and mice heart and is also expressed in fibroblasts and macrophages (31, 32, 34, 57). Studies found that inhibition of SGLT could reduce blood glucose fluctuation in clinical trial (58, 59). Moreover, inhibition of SGLT1 could inactivate human cardiac fibroblasts exposing to HG (34). Knockout of SGLT1 remarkably inhibits the chronic pressure overload-induced cardiac fibrosis through mediating phosphorylation of extracellular signal-regulated kinase (ERK) 1/2 in heart (33). In our study, we found that SGLT1 was upregulated in left ventricular tissues of GVDM mice, IHG-treated RAW264.7 cells, and cardiac fibroblasts. More importantly, inhibition of SGLT1 suppressed macrophage M1 polarization and cardiac fibroblasts activation under conditions of glycemic variability or IHG, which might relieve cardiac dysfunction and fibrosis.

There are some limitations in our study that should be mentioned. Glycemic variability is closer to the actual changes in blood sugar level in diabetic patients (5). The effects of glycemic variability on both diabetes patients and animals are more deleterious than sustained hyperglycemia. Therefore, in this study, we paid more attention to glycemic variability-induced cardiac damage and only inhibited SGLT1 expression in GVDM mice. Additionally, it is well known that SGLT1 is highly expressed in small intestine and regulates the absorption of glucose. We found that SGLT1 was silenced in small intestine, liver, and kidney tissues by shSGLT1, even though the gene silencing efficiency of shSGLT1 seemed higher in heart. However, we found that SGLT1 was

significantly increased in the left ventricular tissues of GVDM mice, the expression of SGLT1 was clearly decreased in left ventricular tissues in GVDM + shSGLT1 mice, and the cardiac fibrosis was improved. Therefore, it is possible that SGLT1 in many organs has synergistic effects for affecting cardiac fibrosis. For instance, knockdown of SGLT1 in small intestine helps to control glucose fluctuation and knockdown of SGLT1 in heart directly inhibits activation of cardiac fibroblasts and macrophage M1 polarization. Additionally, it has been reported that SGLT1 inhibition attenuates apoptosis of cardiomyocyte in diabetic cardiomyopathy animal model and *in vitro* culture (60). We also found that shSGLT1 silenced the expression of SGLT1 in cardiomyocyte in GVDM mice (data not shown). There is a possibility that SGLT1 in cardiomyocyte also plays an important role in glycemic variability-induced cardiac fibrosis. Therefore, we confirmed our hypothesis that SGLT1 mediates the activation of cardiac fibroblasts and macrophages under glucose variability by experiments *in vitro*. The results showed that inhibition of SGLT1 suppressed the cell proliferation and ECM proteins' expression of cardiac fibroblasts and inhibited the M1 polarization of macrophages exposure to IHG. Therefore, our results indicated that SGLT1 in cardiac fibroblasts and macrophages, at least partially, contributes to glycemic variability-induced cardiac fibrosis.

In conclusion, our results indicated that glycemic variability might aggravate cardiac fibrosis by promoting the activation of cardiac fibroblasts and inducing macrophage M1 polarization. Moreover, inhibition of SGLT1 could alleviate the glycemic variability-induced cardiac fibrosis, at least partially, through mediating the activation of macrophage and cardiac fibroblasts.

MATERIALS AND METHODS

Ethical statement. This study was approved by Medical Ethics Committee of the First Affiliated Hospital of Harbin Medical University. All animal experiments referred to the Guide for the Care and Use of Laboratory Animals (61).

Mouse model. The male C57BL/6 mice (18 to 22 g) were purchased from Changsheng Biotechnology Co., Ltd. (China). The mice were randomized into normal and diabetes groups. After 1 week adapting, the mice were fed a high-fat diet (HFD) from weeks 2 to 13, while the control mice were fed a normal diet. Streptozotocin (STZ) (40 mg/kg, S110910, Aladdin, Shanghai, China) was intraperitoneally injected into HFD-fed mice after 6 h fasting for 5 continuous days starting after the last day of week 3. The control mice were given an equal volume of citrate buffer. The fasting blood glucose (FBG) level was measured with a glucometer 72 h after STZ injection. Mice with FBG levels of 16.7 mmol/L or greater were considered to be successful diabetic mice. The diabetic mice then were assigned to the DM, GVDM (glycemic variability in type 2 diabetes mellitus), GVDM + shNC (shRNA-negative control), and GVDM + shSGLT1 (short hairpin RNA targeting SGLT1) groups. All mice from three GVDM groups were subcutaneously injected 20 U/kg insulin (8:00. a.m., 12:00 p.m., and 4:00 p.m.) and intraperitoneally injected 3 g/kg glucose (10:00 a.m., 2:00 p.m., and 6:00 p.m.) every day from weeks 5 to 13. The mice from GVDM + shNC or GVDM + shSGLT1 group were administered 5×10^{10} vector genome (v.g.)/mouse of adeno-associated virus serotype 9 (AAV9, promoter U6)-mediated shSGLT1 or shNC (intravenous injection, Vigene Biosciences, Inc., China) in week 6. The blood glucose levels of mice were measured 30 min after each insulin and glucose injection every day in week 5 to confirm the successful establishment of glycemic variability model. The treatment was stopped at the end of week 13, and the blood glucose levels of mice after each time insulin and glucose injection were measured on the last day of week 13. On the first day of week 14, the cardiac function of mice was determined, and then the mice were directly anesthetized by 5% inhalant isoflurane with an oxygen flow of 1 L/min and then euthanized by cervical dislocation. The experimental process of GVDM induction was shown in Fig. 8A and B. Then left ventricular tissues were collected for pathological and molecular studies. Six mice were used for echocardiography and pathological analysis, and six mice were used for molecular biological analysis. C57BL/6 mice received with AAV9-mediated shSGLT1 or shNC by intravenous injection were used to verify whether shSGLT1 specifically silence SGLT1 in the multiple organs. The heart, kidney, small intestine, and liver tissues of mice were collected 4 weeks later to detect the expression of SGLT1 and SGLT2.

Echocardiography. Cardiac function was analyzed via echocardiography using a Vevo 2100 high-resolution imaging system (VisualSonics Inc., Toronto, Canada) on the last day of the experiment. The mouse was anesthetized using 3% inhalant isoflurane with an oxygen flow of 1 L/min and maintained at 1 to 2% isoflurane during the procedure. The mice were placed in a supine position on a heat pad (38°C) to minimize fluctuations of body temperature. The short-axis M-mode echocardiography was performed, and the following parameters were measured or computed as indicators of left ventricular function: left ventricular end-diastolic dimension (LVEDd), left ventricular end-systolic dimension (LVESd), left ventricular ejection fraction (EF), and fractional shortening (FS).

Histological analysis and immunohistochemical analysis. After fixation with 4% paraformaldehyde, the left ventricular tissues were embedded in paraffin and then cut into 5-μm sections. Subsequently, the sections were deparaffinized and rehydrated. Cardiac fibrosis was evaluated by Masson's trichrome staining. The expression of collagen III was detected by immunohistochemical

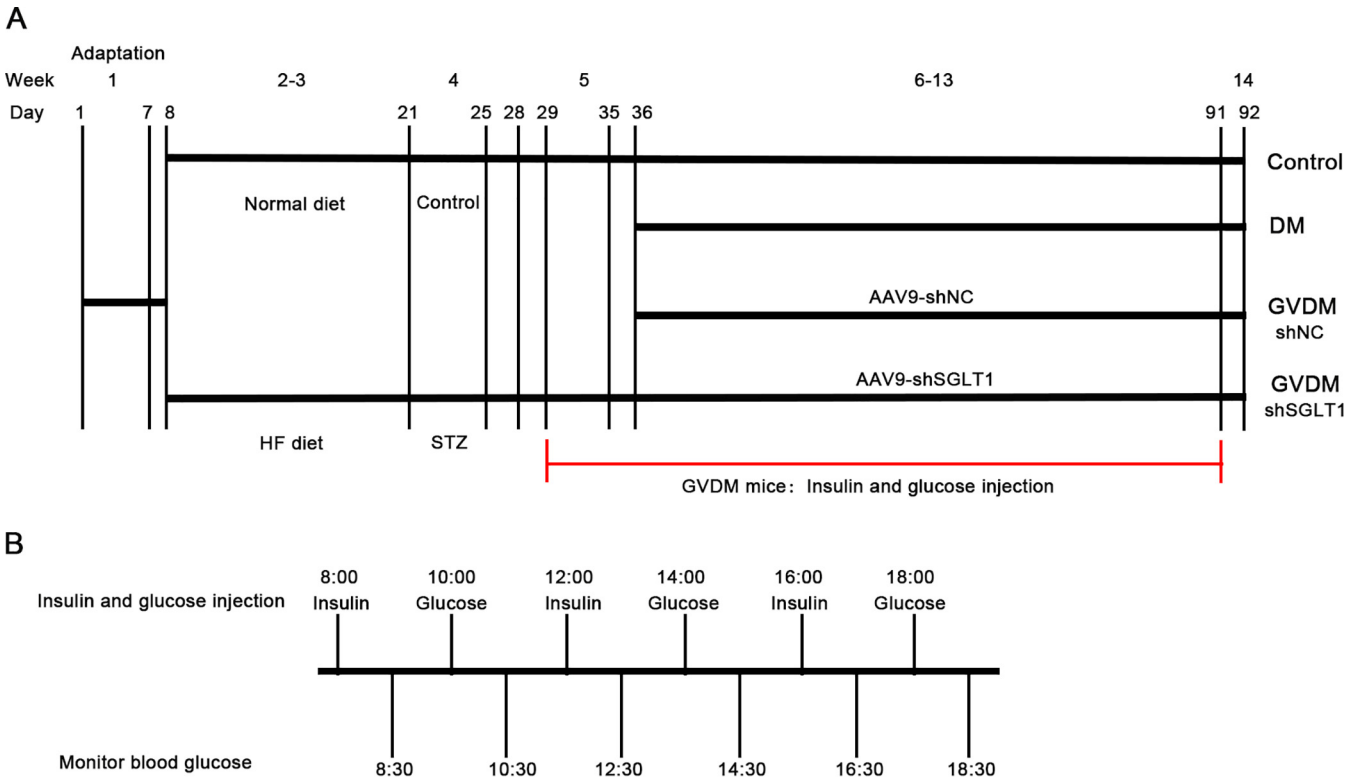

FIG 8 Schematic overview of the GVDM mouse model. (A) Schematic view of the GVDM mice induction and AAV9-shSGLT1 administration in mouse model. (B) Protocol for insulin and glucose injection and blood glucose measurement.

analysis using antibodies against collagen III (AF0136, Affinity, Cincinnati, OH). The results were observed by a microscope with DP73 image analysis program, and three fields of each image were recorded (BX53, Olympus, Tokyo, Japan). For Masson's trichrome staining, the percentage of fibrosis area was calculated using the following formula: percentage of fibrosis area = Aniline Blue staining area/total staining area × 100 (%). For immunohistochemical analysis, the percentage of collagen III expression was calculated using the following formula: percentage of collagen III = anti-collagen III staining area/total staining area × 100 (%).

Immunofluorescence. Double immunofluorescence was performed to evaluate the expression of inducible iNOS (M1 marker) and Arg-1 (arginase 1, M2 marker) on $CD68^+$ macrophages in cardiac tissues. Briefly, the sections were blocked in phosphate-buffered saline (PBS) with goat serum (SL038, Solarbio, Beijing, China) for 15 min. For CD68 and iNOS detection, the sections were incubated with primary antibodies against CD68 (sc-20060, Santa Cruz, CA) and iNOS (AF5369; Affinity) overnight at 4°C. The primary antibodies against CD68 and Arg-1 (DF6657; Affinity) were subsequently used to detect Arg-1 expression in $CD68^+$ macrophages. Subsequently, the sections were washed and incubated with fluorescein isothiocyanate (FITC)-labeled goat anti-mouse IgG (A5608; Beyotime, Shanghai, China) and Cy3-labeled goat anti-rabbit IgG (A0516, Beyotime) for 90 min at room temperature. The identification of the isolated mouse cardiac fibroblasts was performed by immunofluorescence assay, and the cells were stained with anti-vimentin antibody (A2584; Abclonal, Wuhan, China). The results were observed by a microscope under ×400 magnification with the DP73 image analysis program and three fields per each image (BX53). The percentage of iNOS-positive CD68 cells was calculated using the following formula: cell number of iNOS-positive CD68 cells/cell number of CD68-positive cells × 100 (%). The percentage of Arg-1-positive CD68 cells was calculated using the following formula: cell number of Arg-1-positive CD68 cells/cell number of CD68-positive cells × 100 (%). To verify whether SGLT1 is expressed in macrophages and fibroblasts in heart tissue of mice, double immunofluorescence was performed, and the left ventricular tissues of mice from the control, GVDM + shNC, and GVDM + shSGLT1 groups were stained SGLT1 with CD68 or vimentin (a marker of cardiac fibroblasts).

Isolation of cardiac fibroblasts. The thorax was opened to expose the heart of 3- to 4-month-old male C57BL/6 mice. Subsequently, the heart was removed and washed with PBS twice. The aorta was cannulated with an 18-gauge needle and mounted on a Langendorff apparatus. The heart was perfused with a Ca^{2+}-free bicarbonate buffer (pH 7.35) containing 126 mM NaCl, 4.4 mM KCl, 1.0 mM $MgCl_2$, 18 mM $NaHCO_3$, 11 mM glucose, 4 mM HEPES, 10 mM 2,3-butanedione monoxime, and 30 mM taurine at 37°C for 5 min. Then the perfusion buffer was switched to bicarbonate buffer containing 1 mg/mL collagenase II solution, 1 mg/mL albumin, and 2.5 mM $CaCl_2$ for tissue digestion for 20 to 30 min. The digested heart was removed, minced into small pieces, and pipetted to release cells. Then the cells were filtered through a 140-μm-mesh filter to filter out large debris, followed by centrifugation. The cells

TABLE 1 Primer sequences for quantitative real-time PCR

Primer name	Primer sequence (5′ to 3′)
SGLT1 forward	GAGTCTACGCAACAGCAAGG
SGLT1 reverse	AGCCCACAGAACAGGTCATA
iNOS forward	CACCACCCTCCTCGTTC
iNOS reverse	CAATCCACAACTCGCTCC
MCP-1 forward	GCCTGCTGTTCACAGTTGCC
MCP-1 reverse	CTGGACCCATTCCTTCTTGG
CD86 forward	ATGGGCTCGTATGATTGT
CD86 reverse	CTTCTTAGGTTTCGGGTG
CD206 forward	GCAAGTGATTTGGAGGCT
CD206 reverse	ATAGGAAACGGGAGAACC
Arg-1 forward	TATCTGCCAAAGACATCG
Arg-1 reverse	ATCACCTTGCCAATCCC
TGF-β1 forward	TAATGGTGGACCGCAACAAC
TGF-β1 reverse	CACTCAGGCGTATCAGTGGG
β-Actin forward	CTGTGCCCATCTACGAGGGCTAT
β-Actin reverse	TTTGATGTCACGCACGATTTCC

SGLT1, sodium-glucose cotransporter 1; iNOS, inducible nitric-oxide synthase; MCP-1, monocyte chemotactic protein-1; Arg-1, arginase 1; TGF-β1, transforming growth factor β1.

were then resuspended in the Dulbecco's modified Eagle's medium (DMEM; 31600-034, Gibco, Grand Island, NY) supplied with 10% fetal bovine serum (FBS; F8067, Sigma, St. Louis, MO). The cells were cultured at an incubator under 37°C and 5% CO_2. The culture medium was replaced with fresh medium after 4 h of incubation, and the cell identification was performed at the third passage.

Cell culture and treatment. RAW264.7 mouse macrophage cell line was purchased from Zhongqiaoxinzhou (Shanghai, China). RAW264.7 cells and isolated cardiac fibroblasts were cultured in DMEM supplemented with 10% FBS in a 5% CO_2 incubator at 37°C. The cells were seeded with five groups including normal glucose (NG, 5 mM), high glucose (HG, 30 mM), intermittent high glucose (IHG), IHG + shSGLT1, and IHG + shNC. Plasmid Tet-pLKO-puro containing shNC or shSGLT1 were constructed by Nanjing GenScript Co., Ltd. (China). Then the plasmids were expanded and extracted and subjected to virus packaging; the recombinant plasmids were transfected into 293 T cells, respectively; and the cell supernatants were collected 48 h later. Then the supernatants were concentrated by ultracentrifugation to obtain high-titer lentivirus solution. The sequences shRNA targeting SGLT1 or shNC were shSGLT1 (5′-GTGGTGAACATCAACGGTATT-3′) and shNC (5′-TTCTCCGAACGTGTCACGT-3′). For cell infection, cells from IHG + shSGLT1 and IHG + shNC groups were infected with the lentivirus containing shSGLT1 and shNC, respectively. After 24 h, the IHG model was induced. Cells from IHG groups were exposed to HG and NG alternating every 2 h from 8:00 a.m. to 6:00 p.m. and cultured in NG for the rest of the day. The media of the cells from the NG and HG groups were refreshed at the same time point with IHG groups. The cells were analyzed 58 h later after cells from the HG and IHG groups received HG.

MTT. The cardiac fibroblast proliferation was measured using 3-(4,5-dimethylthiazol-2-yl)-2,5-diphenyltetrazolium bromide (MTT). Cardiac fibroblasts (4×10^3) were seeded in 96-well culture plates. Then the MTT assays were performed at 0, 10, 34, and 58 h starting from HG treatment. The culture medium was removed, and the cells were incubated with fresh medium containing 0.5 mg/mL MTT for 4.5 h. Subsequently, the medium was removed, and the formazan crystals were dissolved in 150 μl of dimethyl sulfoxide (DMSO). Then the absorbance of each well was measured at 570 nm using a microplate reader.

RNA preparation and qRT-PCR. Total RNA was extracted from cardiac tissues, cardiac fibroblasts, and RAW264.7 cells using TRIpure reagent (RP1001, BioTeke, Beijing, China) according to the manufacturer's instructions, and reverse transcription was performed to synthesize cDNA. The mRNA expression of SGLT1, transforming growth factor β1 (TGF-β1), iNOS, monocyte chemotactic protein 1 (MCP-1), CD86, CD206, and Arg-1 in cardiac tissues, cardiac fibroblasts, or RAW264.7 cells were measured, and the primer sequences (GenScript, China) were shown in Table 1. The qRT-PCR was performed using an SYBR green (S9430, Sigma), and the mRNA expression of targets was expressed as relative levels to β-actin.

Western blot. Proteins from left ventricle (heart), kidney, small intestine, and liver of mice, cardiac fibroblasts, and RAW264.7 cells were extracted by cell lysis buffer (P0013; Beyotime). The analysis of SDS-PAGE was carried out, and then the proteins were transferred to polyvinylidene difluoride (PVDF) membranes (Millipore, Billerica, MA). After blocking, the membranes were incubated overnight with the primary antibodies with SGLT1 (A11976; Abclonal), SGLT2 (A20271; Abclonal), TGF-β1 (BA0290; Boster, Wuhan, China), collagen I (AF0134; Affinity), collagen III (AF0136; Affinity), fibronectin (AF0738; Affinity), α-SMA (AF1032; Affinity), and β-actin (sc-47778; Santa Cruz). Then the membranes were incubated with secondary antibodies goat anti-rabbit IgG (A0208; Beyotime) or goat anti-mouse IgG (A0216; Beyotime), and the protein bands were visualized by an ECL reagent (P0018; Beyotime) and quantified using gel imaging analysis system with image soft Gel-Pro-Analyzer (WD-9413B; LIUYI, Beijing, China). The densitometric quantitation of SGLT1 was normalized to β-actin, and the relative expression of SGLT1 was normalized to the average level of SGLT1 in the control group.

Data availability. The data are available from the corresponding author on reasonable request.

Statistical analysis. Statistical analysis was performed using Prism 8.0 software (GraphPad Inc., La Jolla, CA). One-way analysis of variance (ANOVA) followed by Tukey's analysis was performed to

compare multiple experimental groups. Two-way ANOVA with repeated measures was used to determine cell proliferation of cardiac fibroblasts. The data are expressed as means ± standard deviation (SD). A value of $P < 0.05$ was considered statistically significant.

ACKNOWLEDGMENTS

This study was funded by National Natural Science Foundation of China grant 81870565.

We declare that there are no potential conflict of interests.

REFERENCES

1. Gude F, Diaz-Vidal P, Rua-Perez C, Alonso-Sampedro M, Fernandez-Merino C, Rey-Garcia J, Cadarso-Suarez C, Pazos-Couselo M, Garcia-Lopez JM, Gonzalez-Quintela A. 2017. Glycemic variability and its association with demographics and lifestyles in a general adult population. J Diabetes Sci Technol 11:780–790. https://doi.org/10.1177/1932296816682031.
2. Chatziralli IP. 2018. The role of glycemic control and variability in diabetic retinopathy. Diabetes Ther 9:431–434. https://doi.org/10.1007/s13300-017-0345-5.
3. Cardoso CRL, Leite NC, Moram CBM, Salles GF. 2018. Long-term visit-to-visit glycemic variability as predictor of micro- and macrovascular complications in patients with type 2 diabetes: the Rio de Janeiro Type 2 Diabetes Cohort Study. Cardiovasc Diabetol 17:33. https://doi.org/10.1186/s12933-018-0677-0.
4. Wang X, Zhao X, Dorje T, Yan H, Qian J, Ge J. 2014. Glycemic variability predicts cardiovascular complications in acute myocardial infarction patients with type 2 diabetes mellitus. Int J Cardiol 172:498–500. https://doi.org/10.1016/j.ijcard.2014.01.015.
5. Bergenstal RM, Ahmann AJ, Bailey T, Beck RW, Bissen J, Buckingham B, Deeb L, Dolin RH, Garg SK, Goland R, Hirsch IB, Klonoff DC, Kruger DF, Matfin G, Mazze RS, Olson BA, Parkin C, Peters A, Powers MA, Rodriguez H, Southerland P, Strock ES, Tamborlane W, Wesley DM. 2013. Recommendations for standardizing glucose reporting and analysis to optimize clinical decision making in diabetes: the Ambulatory Glucose Profile (AGP). Diabetes Technol Ther 15:198–211. https://doi.org/10.1089/dia.2013.0051.
6. Bergenstal RM. 2015. Glycemic variability and diabetes complications: does it matter? Simply put, there are better glycemic markers! Diabetes Care 38:1615–1621. https://doi.org/10.2337/dc15-0099.
7. Umpierrez GE, Kovatchev BP. 2018. Glycemic variability: how to measure and its clinical implication for type 2 diabetes. Am J Med Sci 356:518–527. https://doi.org/10.1016/j.amjms.2018.09.010.
8. Ceriello A, Monnier L, Owens D. 2019. Glycaemic variability in diabetes: clinical and therapeutic implications. Lancet Diabetes Endocrinol 7:221–230. https://doi.org/10.1016/S2213-8587(18)30136-0.
9. Monnier L, Colette C, Owens DR. 2008. Glycemic variability: the third component of the dysglycemia in diabetes. Is it important? How to measure it? J Diabetes Sci Technol 2:1094–1100. https://doi.org/10.1177/193229680800200618.
10. Candido R. 2013. Which patients should be evaluated for blood glucose variability? Diabetes Obes Metab 15:9–12. https://doi.org/10.1111/dom.12141.
11. Monnier L, Mas E, Ginet C, Michel F, Villon L, Cristol JP, Colette C. 2006. Activation of oxidative stress by acute glucose fluctuations compared with sustained chronic hyperglycemia in patients with type 2 diabetes. JAMA 295:1681–1687. https://doi.org/10.1001/jama.295.14.1681.
12. Saisho Y. 2014. Glycemic variability and oxidative stress: a link between diabetes and cardiovascular disease? Int J Mol Sci 15:18381–18406. https://doi.org/10.3390/ijms151018381.
13. Ying C, Zhou X, Chang Z, Ling H, Cheng X, Li W. 2016. Blood glucose fluctuation accelerates renal injury involved to inhibit the AKT signaling pathway in diabetic rats. Endocrine 53:81–96. https://doi.org/10.1007/s12020-016-0867-z.
14. Lu J, Ma X, Zhang L, Mo Y, Ying L, Lu W, Zhu W, Bao Y, Zhou J. 2019. Glycemic variability assessed by continuous glucose monitoring and the risk of diabetic retinopathy in latent autoimmune diabetes of the adult and type 2 diabetes. J Diabetes Invest 10:753–759. https://doi.org/10.1111/jdi.12957.
15. Yokota S, Tanaka H, Mochizuki Y, Soga F, Yamashita K, Tanaka Y, Shono A, Suzuki M, Sumimoto K, Mukai J, Suto M, Takada H, Matsumoto K, Hirota Y, Ogawa W, Hirata KI. 2019. Association of glycemic variability with left ventricular diastolic function in type 2 diabetes mellitus. Cardiovasc Diabetol 18:166. https://doi.org/10.1186/s12933-019-0971-5.
16. Ying C, Liu T, Ling H, Cheng M, Zhou X, Wang S, Mao Y, Chen L, Zhang R, Li W. 2017. Glucose variability aggravates cardiac fibrosis by altering AKT signalling path. Diab Vasc Dis Res 14:327–335. https://doi.org/10.1177/1479164117698917.
17. Yang J, Savvatis K, Kang JS, Fan P, Zhong H, Schwartz K, Barry V, Mikels-Vigdal A, Karpinski S, Kornyeyev D, Adamkewicz J, Feng X, Zhou Q, Shang C, Kumar P, Phan D, Kasner M, Lopez B, Diez J, Wright KC, Kovacs RL, Chen PS, Quertermous T, Smith V, Yao L, Tschope C, Chang CP. 2016. Targeting LOXL2 for cardiac interstitial fibrosis and heart failure treatment. Nat Commun 7:13710. https://doi.org/10.1038/ncomms13710.
18. Henri O, Pouehe C, Houssari M, Galas L, Nicol L, Edwards-Levy F, Henry JP, Dumesnil A, Boukhalfa I, Banquet S, Schapman D, Thuillez C, Richard V, Mulder P, Brakenhielm E. 2016. Selective stimulation of cardiac lymphangiogenesis reduces myocardial edema and fibrosis leading to improved cardiac function following myocardial infarction. Circulation 133:1484–1497. https://doi.org/10.1161/CIRCULATIONAHA.115.020143.
19. Ferrer-Curriu G, Redondo-Angulo I, Guitart-Mampel M, Ruperez C, Mas-Stachurska A, Sitges M, Garrabou G, Villarroya F, Fernandez-Sola J, Planavila A. 2019. Fibroblast growth factor-21 protects against fibrosis in hypertensive heart disease. J Pathol 248:30–40. https://doi.org/10.1002/path.5226.
20. Yue Y, Meng K, Pu Y, Zhang X. 2017. Transforming growth factor beta (TGF-beta) mediates cardiac fibrosis and induces diabetic cardiomyopathy. Diabetes Res Clin Pract 133:124–130. https://doi.org/10.1016/j.diabres.2017.08.018.
21. Lin X, Yang P, Reece EA. 2017. Pregestational type 2 diabetes mellitus induces cardiac hypertrophy in the murine embryo through cardiac remodeling and fibrosis. Am J Obstet Gynecol 217:216.e1–216.e13. https://doi.org/10.1016/j.ajog.2017.04.008. https://doi.org/10.1016/j.ajog.2017.04.008.
22. Zhao T, Chen H, Cheng C, Zhang J, Yan Z, Kuang J, Kong F, Li C, Lu Q. 2019. Liraglutide protects high-glucose-stimulated fibroblasts by activating the CD36-JNK-AP1 pathway to downregulate P4HA1. Biomed Pharmacother 118:109224. https://doi.org/10.1016/j.biopha.2019.109224.
23. Gu X, Fang T, Kang P, Hu J, Yu Y, Li Z, Cheng X, Gao Q. 2017. Effect of ALDH2 on high glucose-induced cardiac fibroblast oxidative stress, apoptosis, and fibrosis. Oxid Med Cell Longev 2017:9257967. https://doi.org/10.1155/2017/9257967.
24. Honold L, Nahrendorf M. 2018. Resident and monocyte-derived macrophages in cardiovascular disease. Circ Res 122:113–127. https://doi.org/10.1161/CIRCRESAHA.117.311071.
25. Rucker AJ, Crowley SD. 2017. The role of macrophages in hypertension and its complications. Pflugers Arch 469:419–430. https://doi.org/10.1007/s00424-017-1950-x.
26. Yang M, Zheng J, Miao Y, Wang Y, Cui W, Guo J, Qiu S, Han Y, Jia L, Li H, Cheng J, Du J. 2012. Serum-glucocorticoid regulated kinase 1 regulates alternatively activated macrophage polarization contributing to angiotensin II-induced inflammation and cardiac fibrosis. Arterioscler Thromb Vasc Biol 32:1675–1686. https://doi.org/10.1161/ATVBAHA.112.248732.
27. Atri C, Guerfali FZ, Laouini D. 2018. Role of human macrophage polarization in inflammation during infectious diseases. Int J Mol Sci 19:1801. https://doi.org/10.3390/ijms19061801. https://doi.org/10.3390/ijms19061801.
28. Jing R, Long TY, Pan W, Li F, Xie QY. 2019. IL-6 knockout ameliorates myocardial remodeling after myocardial infarction by regulating activation of M2 macrophages and fibroblast cells. Eur Rev Med Pharmacol Sci 23:6283–6291. https://doi.org/10.26355/eurrev_201907_18450.
29. Vrhovac I, Eror DB, Klessen D, Burger C, Breljak D, Kraus O, Radović N, Jadrijević S, Aleksic I, Walles T, Sauvant C, Sabolić I, Koepsell H. 2015. Localizations of Na^+-D-glucose cotransporters SGLT1 and SGLT2 in human kidney and of SGLT1 in human small intestine, liver, lung, and

heart. Pflugers Arch 467:1881–1898. https://doi.org/10.1007/s00424-014-1619-7.
30. Rubera I, Poujeol C, Bertin G, Hasseine L, Counillon L, Poujeol P, Tauc M. 2004. Specific Cre/Lox recombination in the mouse proximal tubule. J Am Soc Nephrol 15:2050–2056. https://doi.org/10.1097/01.ASN.0000133023.89251.01.
31. Kashiwagi Y, Nagoshi T, Yoshino T, Tanaka TD, Ito K, Harada T, Takahashi H, Ikegami M, Anzawa R, Yoshimura M. 2015. Expression of SGLT1 in human hearts and impairment of cardiac glucose uptake by phlorizin during ischemia-reperfusion injury in mice. PLoS One 10:e0130605. https://doi.org/10.1371/journal.pone.0130605.
32. Zhou L, Cryan EV, D'Andrea MR, Belkowski S, Conway BR, Demarest KT. 2003. Human cardiomyocytes express high level of Na+/glucose cotransporter 1 (SGLT1). J Cell Biochem 90:339–346. https://doi.org/10.1002/jcb.10631.
33. Matsushita N, Ishida N, Ibi M, Saito M, Sanbe A, Shimojo H, Suzuki S, Koepsell H, Takeishi Y, Morino Y, Taira E, Sawa Y, Hirose M. 2018. Chronic pressure overload induces cardiac hypertrophy and fibrosis via increases in SGLT1 and IL-18 gene expression in mice. Int Heart J 59:1123–1133. https://doi.org/10.1536/ihj.17-565.
34. Meng L, Uzui H, Guo H, Tada H. 2018. Role of SGLT1 in high glucose level-induced MMP-2 expression in human cardiac fibroblasts. Mol Med Rep 17:6887–6892. https://doi.org/10.3892/mmr.2018.8688.
35. Banerjee SK, McGaffin KR, Pastor-Soler NM, Ahmad F. 2009. SGLT1 is a novel cardiac glucose transporter that is perturbed in disease states. Cardiovasc Res 84:111–118. https://doi.org/10.1093/cvr/cvp190.
36. Di Franco A, Cantini G, Tani A, Coppini R, Zecchi-Orlandini S, Raimondi L, Luconi M, Mannucci E. 2017. Sodium-dependent glucose transporters (SGLT) in human ischemic heart: a new potential pharmacological target. Int J Cardiol 243:86–90. https://doi.org/10.1016/j.ijcard.2017.05.032.
37. Sawa Y, Saito M, Ishida N, Ibi M, Matsushita N, Morino Y, Taira E, Hirose M. 2020. Pretreatment with KGA-2727, a selective SGLT1 inhibitor, is protective against myocardial infarction-induced ventricular remodeling and heart failure in mice. J Pharmacol Sci 142:16–25. https://doi.org/10.1016/j.jphs.2019.11.001.
38. Tarbit E, Singh I, Peart JN, Rose'Meyer RB. 2019. Biomarkers for the identification of cardiac fibroblast and myofibroblast cells. Heart Fail Rev 24:1–15. https://doi.org/10.1007/s10741-018-9720-1.
39. Jin L, Sun S, Ryu Y, Piao ZH, Liu B, Choi SY, Kim GR, Kim HS, Kee HJ, Jeong MH. 2018. Gallic acid improves cardiac dysfunction and fibrosis in pressure overload-induced heart failure. Sci Rep 8:9302. https://doi.org/10.1038/s41598-018-27599-4.
40. Frangogiannis NG. 2015. Pathophysiology of myocardial infarction. Compr Physiol 5:1841–1875. https://doi.org/10.1002/cphy.c150006.
41. Jia G, DeMarco VG, Sowers JR. 2016. Insulin resistance and hyperinsulinaemia in diabetic cardiomyopathy. Nat Rev Endocrinol 12:144–153. https://doi.org/10.1038/nrendo.2015.216.
42. Saito S, Teshima Y, Fukui A, Kondo H, Nishio S, Nakagawa M, Saikawa T, Takahashi N. 2014. Glucose fluctuations increase the incidence of atrial fibrillation in diabetic rats. Cardiovasc Res 104:5–14. https://doi.org/10.1093/cvr/cvu176.
43. Weiskirchen R, Weiskirchen S, Tacke F. 2019. Organ and tissue fibrosis: molecular signals, cellular mechanisms and translational implications. Mol Aspects Med 65:2–15. https://doi.org/10.1016/j.mam.2018.06.003.
44. Kong P, Christia P, Frangogiannis NG. 2014. The pathogenesis of cardiac fibrosis. Cell Mol Life Sci 71:549–574. https://doi.org/10.1007/s00018-013-1349-6.
45. Nishikawa K. 1998. Angiotensin AT1 receptor antagonism and protection against cardiovascular end-organ damage. J Hum Hypertens 12:301–309. https://doi.org/10.1038/sj.jhh.1000634.
46. Lei B, Hitomi H, Mori T, Nagai Y, Deguchi K, Mori H, Masaki T, Nakano D, Kobori H, Kitaura Y, Nishiyama A. 2011. Effect of efonidipine on TGF-β1-induced cardiac fibrosis through Smad2-dependent pathway in rat cardiac fibroblasts. J Pharmacol Sci 117:98–105. https://doi.org/10.1254/jphs.11065fp.
47. Jin D, Han F. 2020. FOXF1 ameliorates angiotensin II-induced cardiac fibrosis in cardiac fibroblasts through inhibiting the TGF-β1/Smad3 signaling pathway. J Recept Signal Transduct Res 40:493–500. https://doi.org/10.1080/10799893.2020.1772299.
48. Zeng Z, Wang Q, Yang X, Ren Y, Jiao S, Zhu Q, Guo D, Xia K, Wang Y, Li C, Wang W. 2019. Qishen granule attenuates cardiac fibrosis by regulating TGF-β/Smad3 and GSK-3β pathway. Phytomedicine 62:152949. https://doi.org/10.1016/j.phymed.2019.152949.
49. Liu JC, Wang F, Xie ML, Cheng ZQ, Qin Q, Chen L, Chen R. 2017. Osthole inhibits the expressions of collagen I and III through Smad signaling pathway after treatment with TGF-β1 in mouse cardiac fibroblasts. Int J Cardiol 228:388–393. https://doi.org/10.1016/j.ijcard.2016.11.202.
50. Jiang L, Chen FX, Zang ST, Yang QF. 2017. Betulinic acid prevents high glucose-induced expression of extracellular matrix protein in cardiac fibroblasts by inhibiting the TGF-β1/Smad signaling pathway. Mol Med Rep 16:6320–6325. https://doi.org/10.3892/mmr.2017.7323.
51. Yuan H, Xu J, Xu X, Gao T, Wang Y, Fan Y, Hu J, Shao Y, Zhao B, Li H, Sun J, Xu C. 2019. Calhex^{231} alleviates high glucose-induced myocardial fibrosis via inhibiting itch-ubiquitin proteasome pathway in vitro. Biol Pharm Bull 42:1337–1344. https://doi.org/10.1248/bpb.b19-00090.
52. Kanda H, Tateya S, Tamori Y, Kotani K, Hiasa K, Kitazawa R, Kitazawa S, Miyachi H, Maeda S, Egashira K, Kasuga M. 2006. MCP-1 contributes to macrophage infiltration into adipose tissue, insulin resistance, and hepatic steatosis in obesity. J Clin Invest 116:1494–1505. https://doi.org/10.1172/JCI26498.
53. Tsutsumi-Kuroda U, Inoue T, Futakuchi A, Shobayashi K, Takahashi E, Kojima S, Inoue-Mochita M, Fujimoto T, Tanihara H. 2018. Decreased MCP-1/CCR2 axis-mediated chemotactic effect of conjunctival fibroblasts after transdifferentiation into myofibroblasts. Exp Eye Res 170:76–80. https://doi.org/10.1016/j.exer.2018.02.008.
54. Gharaee-Kermani M, Denholm EM, Phan SH. 1996. Costimulation of fibroblast collagen and transforming growth factor beta1 gene expression by monocyte chemoattractant protein-1 via specific receptors. J Biol Chem 271:17779–17784. https://doi.org/10.1074/jbc.271.30.17779.
55. Castilla-Madrigal R, Gil-Iturbe E, Sáinz N, Moreno-Aliaga MJ, Lostao MP. 2019. Basolateral presence of the proinflammatory cytokine tumor necrosis factor -α and secretions from adipocytes and macrophages reduce intestinal sugar transport. J Cell Physiol 234:4352–4361. https://doi.org/10.1002/jcp.27216.
56. Rizzo MR, Barbieri M, Marfella R, Paolisso G. 2012. Reduction of oxidative stress and inflammation by blunting daily acute glucose fluctuations in patients with type 2 diabetes: role of dipeptidyl peptidase-IV inhibition. Diabetes Care 35:2076–2082. https://doi.org/10.2337/dc12-0199.
57. Notari L, Riera DC, Sun R, Bohl JA, McLean LP, Madden KB, van Rooijen N, Vanuytsel T, Urban JF, Jr, Zhao A, Shea-Donohue T. 2014. Role of macrophages in the altered epithelial function during a type 2 immune response induced by enteric nematode infection. PLoS One 9:e84763. https://doi.org/10.1371/journal.pone.0084763.
58. Danne T, Cariou B, Buse JB, Garg SK, Rosenstock J, Banks P, Kushner JA, McGuire DK, Peters AL, Sawhney S, Strumph P. 2019. Improved time in range and glycemic variability with sotagliflozin in combination with insulin in adults with type 1 diabetes: a pooled analysis of 24-week continuous glucose monitoring data from the inTandem program. Dia Care 42:919–930. https://doi.org/10.2337/dc18-2149.
59. Danne T, Garg S, Peters AL, Buse JB, Mathieu C, Pettus JH, Alexander CM, Battelino T, Ampudia-Blasco FJ, Bode BW, Cariou B, Close KL, Dandona P, Dutta S, Ferrannini E, Fourlanos S, Grunberger G, Heller SR, Henry RR, Kurian MJ, Kushner JA, Oron T, Parkin CG, Pieber TR, Rodbard HW, Schatz D, Skyler JS, Tamborlane WV, Yokote K, Phillip M. 2019. International consensus on risk management of diabetic ketoacidosis in patients with type 1 diabetes treated with sodium-glucose cotransporter (SGLT) inhibitors. Diabetes Care 42:1147–1154. https://doi.org/10.2337/dc18-2316.
60. Lin N, Lin H, Yang Q, Lu W, Sun Z, Sun S, Meng L, Chi J, Guo H. 2020. SGLT1 inhibition attenuates apoptosis in diabetic cardiomyopathy via the JNK and p38 pathway. Front Pharmacol 11:598353. https://doi.org/10.3389/fphar.2020.598353.
61. National Research Council Committee for the Update of the Guide for the Care and Use of Laboratory Animals. 2011. Guide for the care and use of laboratory animals, 8th ed. National Academies Press, Washington, DC.